

MICROBIOTA

The intestinal microbiota regulates body composition through NFIL3 and the circadian clock

Yuhao Wang,¹ Zheng Kuang,¹ Xiaofei Yu,^{1*} Kelly A. Ruhn,¹ Masato Kubo,^{2,3} Lora V. Hooper^{1,4†}

The intestinal microbiota has been identified as an environmental factor that markedly affects energy storage and body-fat accumulation in mammals, yet the underlying mechanisms remain unclear. Here we show that the microbiota regulates body composition through the circadian transcription factor NFIL3. *Nfil3* transcription oscillates diurnally in intestinal epithelial cells, and the amplitude of the circadian oscillation is controlled by the microbiota through group 3 innate lymphoid cells, STAT3 (signal transducer and activator of transcription 3), and the epithelial cell circadian clock. NFIL3 controls expression of a circadian lipid metabolic program and regulates lipid absorption and export in intestinal epithelial cells. These findings provide mechanistic insight into how the intestinal microbiota regulates body composition and establish NFIL3 as an essential molecular link among the microbiota, the circadian clock, and host metabolism.

The worldwide obesity epidemic presents a pressing public health crisis. More than 2.1 billion individuals throughout the world are overweight or obese, and ~3.4 million deaths per year are caused by obesity-related diseases (1). Consequently, there is an urgent need to identify host and environmental factors that regulate human metabolism and energy homeostasis.

The intestinal microbiota is an environmental factor that markedly affects mammalian body composition. The microbiota promotes energy storage in adipose tissue, and thus microbiologically

sterile (germ-free) mice have less body fat relative to conventionally raised mice (2). This is because, in part, the microbiota enhance energy harvest from the host diet (3) and promote storage of that energy in adipose tissue (2). Less is known about how microbial regulation of host metabolic pathways might also affect energy storage and body composition.

Many host metabolic pathways are synchronized with day-night light cycles through the circadian clock. The mammalian circadian clock is a network of transcription factors, present in all cells of the body, that drives rhythmic ~24-hour

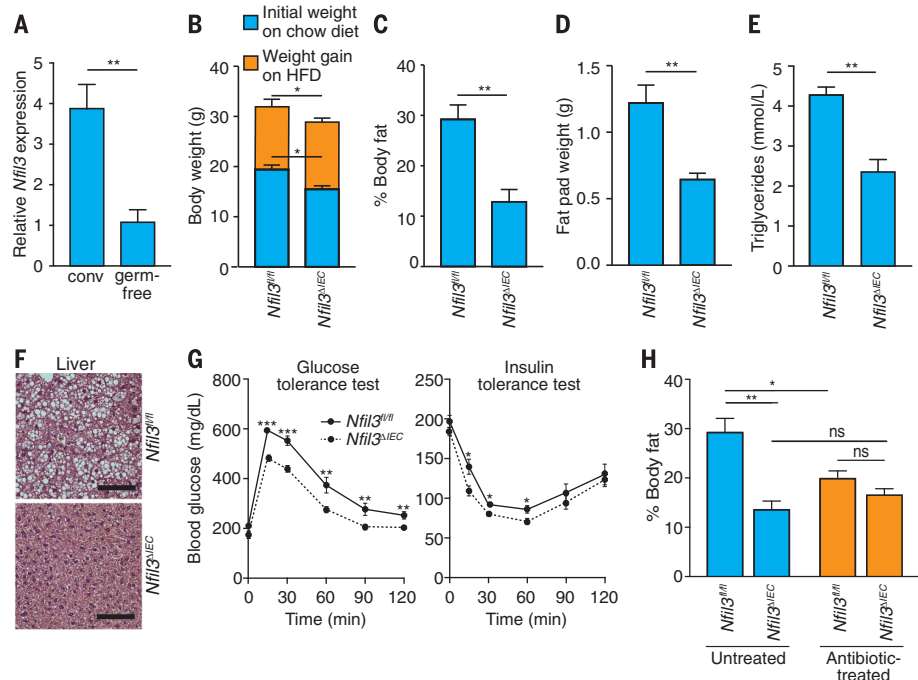
oscillations in gene expression. Synchronization of metabolism with the clock couples energetically expensive metabolic pathways to the availability of dietary substrates, optimizing energy utilization. Emerging evidence indicates that the microbiota interacts with the circadian clock in ways that profoundly affect host metabolism and that disrupting these interactions can lead to obesity and other metabolic diseases (4, 5). However, little is known about the mechanisms that govern microbiota interactions with the circadian clock and how these interactions alter host metabolism.

NFIL3, also known as E4BP4, is a basic leucine zipper transcription factor that is expressed in a variety of immune cells and controls immune functions that vary by cell type (6, 7). We found that small intestinal epithelial cells also expressed NFIL3 and that expression was markedly reduced in germ-free mice (Fig. 1A). This accorded with earlier findings in antibiotic-treated mice (8) and suggested that epithelial NFIL3 might regulate a physiological activity that is responsive to the intestinal microbiota.

To identify the physiological functions of NFIL3 in intestinal epithelial cells, we generated an

Fig. 1. *Nfil3*^{MEC} mice are resistant to high-fat diet-induced obesity.

(A) qRT-PCR analysis of *Nfil3* transcript abundance in small intestinal epithelial cells recovered by laser capture microdissection from conventional (conv) and germ-free mice. (B) Age-matched *Nfil3*^{fl/fl} and *Nfil3*^{MEC} mice were cohoused and placed on a high-fat diet (HFD) for 10 weeks. Body weight was measured before and after diet switching. (C) Body-fat percentages of mice in (B). (D) Epididymal fat-pad weight. (E) Serum triglyceride concentration. (F) Hematoxylin and eosin (H&E) staining of liver (scale bars, 100 μ m). (G) Glucose-tolerance and insulin-tolerance tests. (H) Body-fat percentage of mice treated with or without antibiotics after switching to a HFD. All data represent two independent experiments with four to eight mice per group. Male mice were used in all experiments. Means \pm SEM (error bars) are plotted; statistics were performed with Student's *t* test or one-way analysis of variance (ANOVA). **P* < 0.05; ***P* < 0.01; ****P* < 0.001; ns, not significant.



epithelial cell-specific *Nfil3* knockout mouse (*Nfil3^{ΔIEC}*). *Nfil3^{ΔIEC}* mice raised on a chow diet weighed less than their *Nfil3^{fl/fl}* littermates (Fig. 1B and fig. S1A) and had reduced body fat and increased lean body mass relative to *Nfil3^{fl/fl}* littermates (fig. S1, B and C). The body composition differences were not due to off-target effects of CRE expression (fig. S1, D and E) or differences in food intake (fig. S2A), physical activity (fig. S2B), or energy utilization (fig. S3, A to C), which were similar between the two groups. We also did not detect differences in the response to intestinal

injury (fig. S4, A to D) or in the expression of key inflammatory cytokines and antimicrobial proteins (fig. S5, A to E).

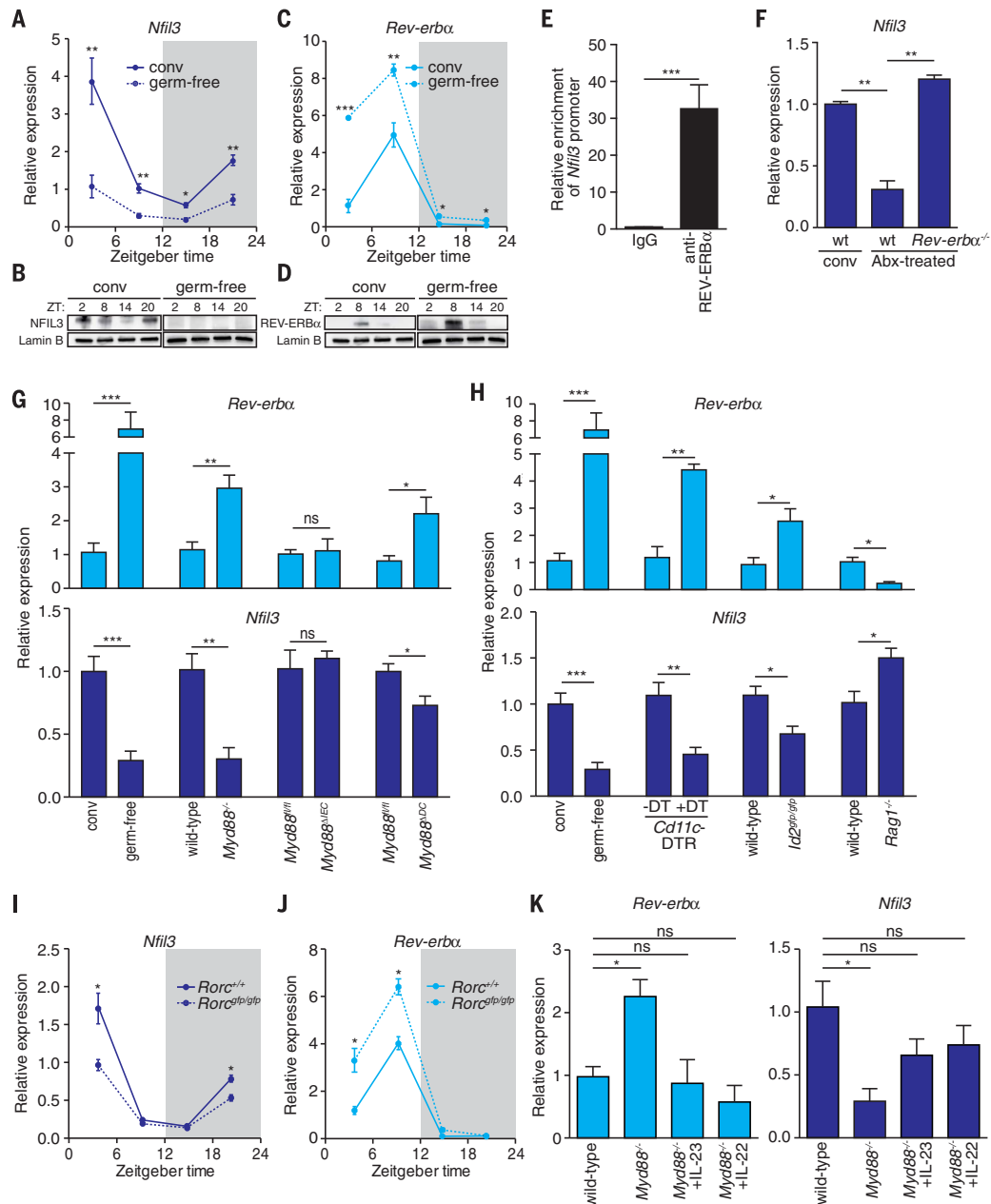
When placed on a high-fat, Western-style diet (HFD) for 10 weeks, both *Nfil3^{fl/fl}* and *Nfil3^{ΔIEC}* mice gained weight (Fig. 1B). However, the *Nfil3^{ΔIEC}* mice maintained lower body weights (Fig. 1B) and had lower body-fat percentages (Fig. 1C) and higher lean-body-mass percentages (fig. S6A). The *Nfil3^{ΔIEC}* mice also had lower epididymal fat-pad weights (Fig. 1D and fig. S6B) and were protected from elevated blood triglycerides (Fig. 1E), liver-fat

accumulation (Fig. 1F), lowered glucose tolerance (Fig. 1G), and increased insulin resistance (Fig. 1G). 16S ribosomal RNA gene sequencing of fecal microbiotas indicated that the metabolic differences between *Nfil3^{fl/fl}* and *Nfil3^{ΔIEC}* mice were not due to differences in microbiota taxonomic composition (fig. S7). Thus, epithelial *NFIL3* regulates lipid storage and body composition in mice.

Because epithelial *NFIL3* expression is dependent on the microbiota, we sought to determine whether *NFIL3*-dependent body-fat accumulation

Fig. 2. The microbiota induces epithelial *NFIL3* expression through the circadian clock factor *REV-ERB α* and a DC-ILC3 signaling relay.

(A to D) qRT-PCR analysis of *Nfil3* (A) and *Rev-erba* (C) transcript abundance in small intestinal epithelial cells from germ-free (dotted line) and conventional (solid line) mice across a 24-hour day-night light cycle. Western blot analysis of *NFIL3* (B) and *REV-ERB α* (D) was performed on small intestinal epithelial cells isolated from conventional or germ-free mice. Lamin B was used as the loading control. ZT, Zeitgeber time. (E) Chromatin immunoprecipitation assay on intestinal epithelial cells using immunoglobulin G (IgG) or an antibody to *REV-ERB α* (anti-*REV-ERB α*). Precipitated fragments of the *Nfil3* promoter were detected by qRT-PCR. (F) qRT-PCR analysis of epithelial *Nfil3* expression in conventional (conv) wild-type (wt), antibiotic (Abx)-treated wild-type, or Abx-treated *Rev-erba^{-/-}* mice. (G) qRT-PCR analysis of epithelial *Rev-erba* and *Nfil3* expression in germ-free and conventional wild-type mice and conventional *Myd88^{fl/fl}*, *Myd88^{-/-}*, *Myd88^{ΔIEC}* (epithelial cell-specific knockout), and *Myd88^{ΔDC}* (DC-specific knockout) mice. (H) qRT-PCR analysis of epithelial *Rev-erba* and *Nfil3* expression in germ-free and conventional wild-type mice, conventional *Cd11c-DTR* mice that were untreated or treated with *Diphtheria toxin* (DT), *Id2^{gfp/gfp}* mice, and *Rag1^{-/-}* mice. (I and J) qRT-PCR analysis of epithelial *Nfil3* (I) and *Rev-erba* (J) expression in *Rorc^{+/+}* (solid line) and *Rorc^{gfp/gfp}* (dotted line) mice. (K) qRT-PCR analysis of epithelial *Rev-erba* and *Nfil3* expression in *Myd88^{-/-}* mice treated with recombinant IL-23, IL-22, or vehicle. Data in (E), (F), (G), (H), and (K) were collected at ZT4. $N = 3$ to 8 mice per group. Means \pm SEM (error bars) are plotted; statistics were performed with Student's *t* test or one-way ANOVA. * $P < 0.05$; ** $P < 0.01$; *** $P < 0.001$; ns, not significant.



also depends on the microbiota. Depletion of the microbiota through antibiotic treatment produced lower fat and higher lean body mass in the *Nfil3^{fl/fl}* mice, resulting in body compositions that were not significantly different from those of *Nfil3^{ΔIEC}* mice (Fig. 1H and fig. S8). Thus, HFD-induced body-fat accumulation requires both NFIL3 and a microbiota.

We next studied the mechanism by which the microbiota regulates NFIL3 expression. *Nfil3* transcription is controlled by the circadian clock (9); accordingly, *Nfil3* transcript abundance oscillated diurnally in an enriched population of small intestinal epithelial cells acquired by laser capture microdissection (Fig. 2A). Comparison of *Nfil3* expression levels across a circadian cycle in wild-type germ-free and conventional mice revealed that the microbiota is required for maximal *Nfil3* expression and thus governs the amplitude of *Nfil3* transcriptional rhythms (Fig. 2A). This was reflected in protein expression levels (Fig. 2B) and accords with earlier findings in antibiotic-treated mice (8).

Nfil3 expression is directly regulated by the core circadian clock transcriptional repressor REV-ERBa. In T cells and liver cells, REV-ERBa binds to a consensus sequence in the *Nfil3* gene locus and represses transcription, resulting in a rhythmic diurnal *Nfil3* expression pattern (6, 10). *Rev-erba* transcript and protein abundance also oscillated diurnally in intestinal epithelial cells but was higher in germ-free mice versus conventional mice (Fig. 2, C and D). This suggested that REV-ERBa governs circadian rhythmicity in *Nfil3* expression and that the microbiota might induce *Nfil3* expression by repressing *Rev-erba* expression. REV-ERBa bound directly to the *Nfil3* promoter in intestinal epithelial cells, as assessed by chromatin immunoprecipitation (ChIP) assay (Fig. 2E). Further, *Nfil3* expression in antibiotic-treated *Rev-erba^{-/-}* mice was similar to that in conventional wild-type mice (Fig. 2F). Thus, microbiota regulation of *Nfil3* expression is REV-ERBa-dependent, and the microbiota elevates *Nfil3* expression by repressing *Rev-erba* expression.

We next sought to determine how bacterial signals are relayed to the epithelial circadian clock to regulate *Rev-erba* and *Nfil3* expression. Intestinal epithelial cells sense the microbiota through Toll-like receptors (TLRs) and their common signaling adaptor MyD88 to regulate the expression of key genes (11). We therefore tested whether MyD88 is required for microbiota regulation of *Rev-erba* and *Nfil3* expression in epithelial cells. We quantified *Rev-erba* and *Nfil3* transcripts in epithelial cells from *Myd88^{-/-}* mice and wild-type littermates at Zeitgeber time 4 (ZT4), which is when *Nfil3* expression is near-peak in conventional mice (Fig. 2A). Epithelial *Rev-erba* expression was increased and *Nfil3* expression was consequently reduced to germ-free levels in *Myd88^{-/-}* mice (Fig. 2G), indicating that microbiota regulation of the *Rev-erba*-*Nfil3* cascade requires MyD88. Whereas epithelial MyD88 was dispensable for microbiota-induced alterations in *Rev-erba* and *Nfil3* expression, *Myd88*

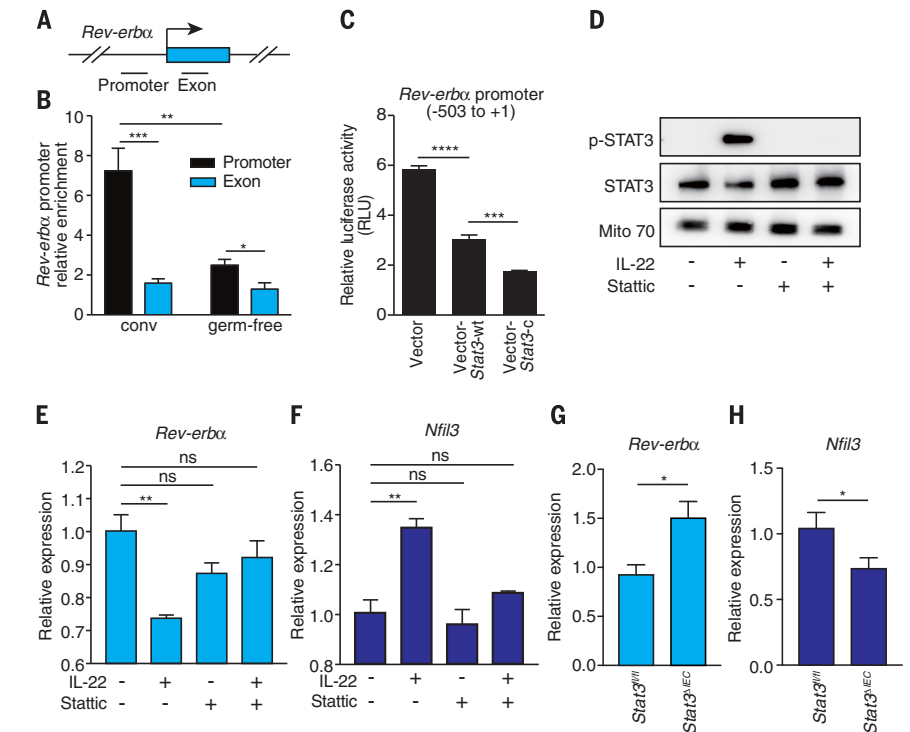


Fig. 3. STAT3 represses *Rev-erba* transcription by binding directly to its promoter. (A) Schematic of the *Rev-erba* gene promoter. (B) ChIP analysis of intestinal epithelial cells from conventional or germ-free mice using IgG or anti-STAT3 antibody. Precipitated fragments of the *Rev-erba* promoter or control exon were detected by qRT-PCR. (C) Luciferase reporter assay. A 504-bp fragment of the *Rev-erba* promoter was fused to a firefly luciferase reporter. HEK-293T cells were transfected with reporters and empty vector, a wild-type STAT3-encoding vector (*Stat3-wt*), or a dominant active STAT3-encoding vector (*Stat3-c*). RLU, relative light units. (D) Western-blot of total STAT3 and phosphorylated STAT3 (p-STAT3) in small intestinal organoids treated with IL-22 and/or the STAT3 inhibitor Stattic. Mito 70 was used as the loading control. (E and F) qRT-PCR analysis of *Rev-erba* (E) and *Nfil3* (F) expression in small intestinal organoids treated with IL-22 and/or Stattic. (G and H) qRT-PCR analysis of epithelial *Rev-erba* (G) and *Nfil3* (H) expression in *Stat3^{fl/fl}* and *Stat3^{MEC}* mice at ZT4. $N = 3$ to 8 samples per group. Means \pm SEM (error bars) are plotted; statistics were performed with Student's t test or one-way ANOVA. * $P < 0.05$; ** $P < 0.01$; *** $P < 0.001$; **** $P < 0.0001$; ns, not significant.

expression in a CD11c⁺ cell population (which includes some dendritic cells) was required for maximal repression of *Rev-erba* and induction of *Nfil3* (Fig. 2G), suggesting a requirement for dendritic cells (DCs).

To further test for DC involvement, we used a mouse model of DC depletion in which *Diphtheria* toxin receptor (DTR) is expressed under the control of the *Cd11c* promoter (12). On administration of *Diphtheria* toxin, CD11c⁺ cells are selectively killed (12). On CD11c⁺ cell depletion, *Rev-erba* expression was increased and *Nfil3* expression was decreased (Fig. 2H), supporting a requirement for DCs in microbiota induction of *Nfil3*.

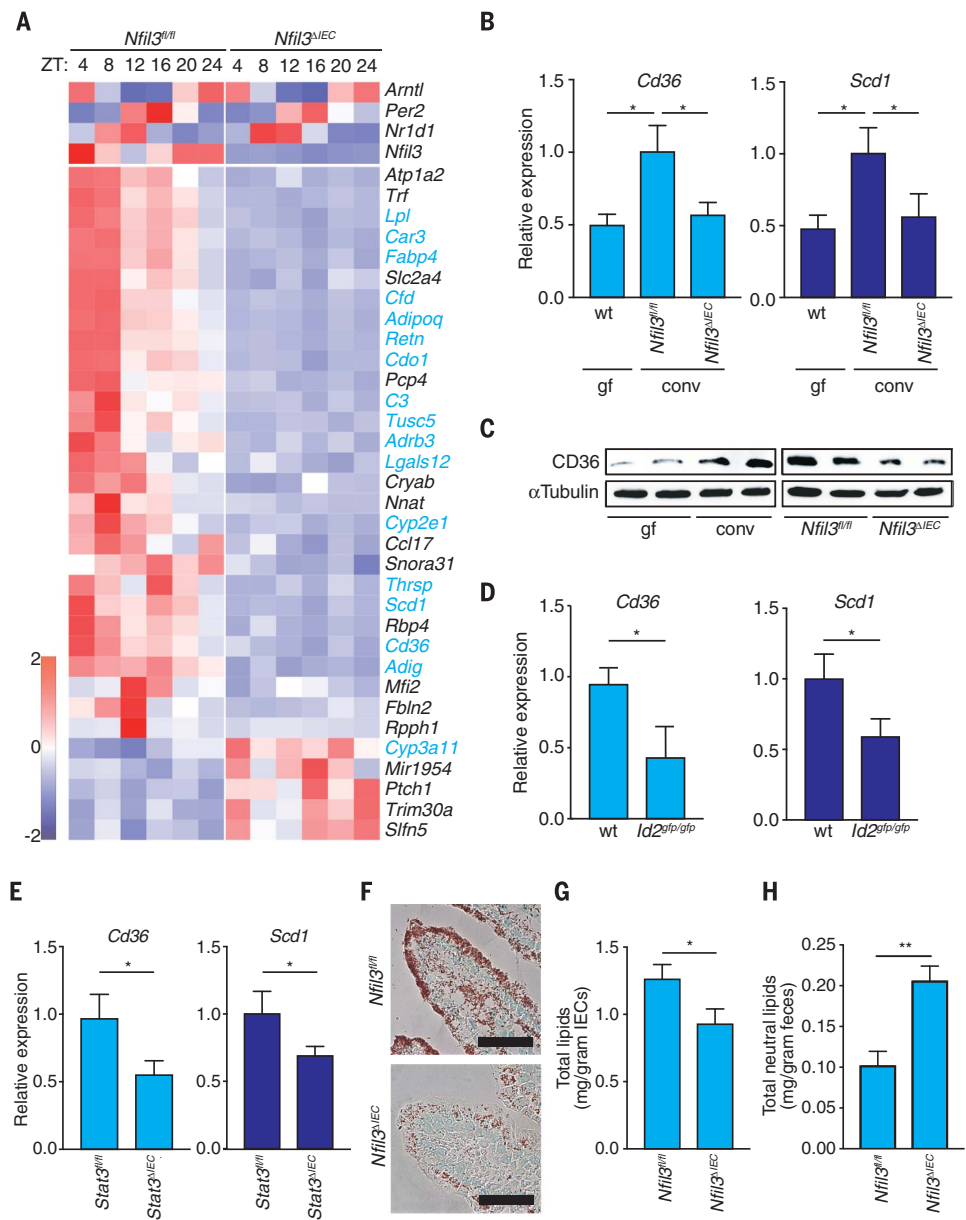
Previous studies have identified a subepithelial cellular signaling relay in the small intestine that captures microbiota signals and passes them to epithelial cells to alter expression of key epithelial cell genes (13, 14). In this circuit, bacteria activate TLR-MyD88 signaling in DCs, and the bacterial signals are relayed from DC to group 3

innate lymphoid cells (ILC3) through the cytokine interleukin-23 (IL-23). ILC3 then signal to the epithelium through the production of IL-22 (15).

To determine whether ILCs were required for microbiota-induced *Nfil3* expression, we studied ID2-deficient mice (*Id2^{gfp/gfp}*), which lack all known ILC subsets (16, 17). *Id2^{gfp/gfp}* mice showed increased *Rev-erba* expression and consequent decreased *Nfil3* expression in the small intestinal epithelium (Fig. 2H), consistent with a requirement for ILCs in regulating *Rev-erba* expression. *Rag1^{-/-}* mice, which lack T and B cells, showed decreased epithelial *Rev-erba* expression and increased *Nfil3* expression (Fig. 2H). The fact that *Nfil3* expression was higher in *Rag1^{-/-}* mice than in conventional wild-type mice is likely due to the elevated bacterial loads as well as aberrant expansion of ILC3 in the small intestines of these mice (18) and indicates that T and B cells are not required for induction of *Nfil3* expression. ROR γ t-deficient (*Rorc^{gfp/gfp}*) mice

Fig. 4. Epithelial NFIL3 controls expression of a circadian lipid metabolic program and regulates lipid absorption in intestinal epithelial cells.

(A) RNA sequencing analysis of epithelial cell transcripts in *Nfil3^{fl/fl}* and *Nfil3^{ΔIEC}* mice across a circadian cycle. The heat map displays expression levels of the 33 genes that have altered expression in *Nfil3^{ΔIEC}* mice as compared with *Nfil3^{fl/fl}* mice. Genes encoding proteins that function in lipid metabolism are highlighted in blue. Top panels show sustained circadian expression of the core clock genes *Bmal1* (*Arntl*), *Per2*, and *Nr1d1* (*Rev-erba*) in *Nfil3^{ΔIEC}* mice. **(B)** qRT-PCR analysis of epithelial *Cd36* and *Scd1* expression in germ-free wild-type and conventional *Nfil3^{fl/fl}* and *Nfil3^{ΔIEC}* mice at ZT4. **(C)** Western blot of epithelial CD36 in germ-free (gf) and conventional wild-type (conv) mice, as well as in conventional *Nfil3^{fl/fl}* and *Nfil3^{ΔIEC}* mice. All mice were fed a HFD. Mice were sacrificed at ZT4. α -Tubulin was used as the loading control. **(D)** and **(E)** qRT-PCR analysis of epithelial *Cd36* and *Scd1* expression in conventional wild-type (wt) and ID2-deficient (*Id2^{gfp/gfp}*) mice (D) and *Stat3^{fl/fl}* and *Stat3^{ΔIEC}* mice (E) at ZT4. **(F)** Oil Red O detection of lipids in the small intestines of *Nfil3^{fl/fl}* and *Nfil3^{ΔIEC}* mice fed a HFD. Nuclei were stained with methyl green. Scale bars, 40 μ m. **(G)** Total lipid concentrations in isolated small intestinal epithelial cells (IECs) from *Nfil3^{fl/fl}* and *Nfil3^{ΔIEC}* mice fed a HFD. **(H)** Total neutral lipid concentrations in feces of *Nfil3^{fl/fl}* and *Nfil3^{ΔIEC}* mice fed a HFD. Data in (B), (D), (E), (G), and (H) are from *N* = 5 to 12 mice per group. Means \pm SEM (error bars) are plotted; statistics were performed with Student's *t* test or one-way ANOVA. **P* < 0.05; ***P* < 0.01.



(19), which lack both T helper 17 cells and ILC3, showed circadian *Rev-erba* and *Nfil3* expression patterns (Fig. 2, I and J) that were similar to those of germ-free mice (Fig. 2, A and B). This establishes that ILC3 are required for microbiota induction of *Nfil3* expression through *Rev-erba*. Treatment of *Myd88^{-/-}* mice with recombinant IL-23 or IL-22 restored epithelial *Rev-erba* and *Nfil3* expression to wild-type conventional levels (Fig. 2K), further supporting the idea that the subepithelial DC-ILC3 circuit relays microbiota signals to epithelial cells to regulate *Nfil3* expression.

The intestinal DC-ILC3 circuit can be triggered by flagellin or lipopolysaccharide (LPS), which is present in the outer membranes of Gram-negative bacteria (20, 21). Accordingly, treatment of germ-free mice with flagellin and LPS decreased

Rev-erba expression and increased *Nfil3* expression (fig. S9, A and B). Further, *Rev-erba* expression decreased and *Nfil3* expression increased when we monoassociated germ-free mice with Gram-negative, flagellated bacterial species, including *Salmonella typhimurium* and *Escherichia coli* (fig. S9, A and B). *Rev-erba* and *Nfil3* expression were not markedly altered by monoassociation with the Gram-positive species *Enterococcus faecalis* or with the Gram-negative nonflagellated species *Bacteroides thetaiotaomicron*, suggesting that *Nfil3* expression is selectively activated by Gram-negative, motile bacteria. This is likely because such bacteria produce both flagellin and LPS and because they can readily penetrate the intestinal epithelial barrier and contact lamina propria DCs.

We next sought to identify epithelial cell-intrinsic pathways downstream of IL-22 that

regulate *Rev-erba* and *Nfil3* expression. The transcription factor STAT3 (signal transducer and activator of transcription 3) is a key response element downstream of the IL-22 receptor (IL-22R) (14). Activation of the IL-22R leads to phosphorylation of STAT3, which then binds to the promoters of its target genes and either activates or inhibits their transcription. ChIP analysis of intestinal epithelial cells showed STAT3 binding to the *Rev-erba* promoter (Fig. 3, A and B). STAT3 binding was markedly reduced in epithelial cells from germ-free mice (Fig. 3, A and B). Cotransfection of STAT3-encoding vectors with luciferase reporters fused to the *Rev-erba* promoter resulted in decreased luciferase activity in human embryonic kidney-293 T (HEK-293T) cells (Fig. 3C), and expression of a dominant active form of STAT3 further inhibited the luciferase activity

(Fig. 3C). Thus, STAT3 binds to the *Rev-erba* promoter and inhibits its transcription.

We used cultured intestinal organoids to further evaluate the role of STAT3 in repressing *Rev-erba* transcription. Addition of recombinant IL-22 to organoid cultures resulted in STAT3 phosphorylation (Fig. 3D), supporting earlier findings that IL-22 activates STAT3 in intestinal epithelial cells (14). At the same time, expression of *Rev-erba* was decreased and expression of *Nfil3* was increased as compared with controls (Fig. 3, E and F). In contrast, when we added a STAT3 phosphorylation inhibitor (Stattic) (22) to organoids, together with recombinant IL-22, STAT3 phosphorylation was inhibited (Fig. 3D), and *Rev-erba* and *Nfil3* showed expression levels similar to those of the controls (Fig. 3, E and F). These findings further support the idea that STAT3 is a transcriptional repressor of *Rev-erba*.

We next investigated whether STAT3 is required for microbiota repression of epithelial *Rev-erba* expression in vivo. We generated a mouse with an epithelial cell-specific deletion of *Stat3* (*Stat3^{ΔIEC}*) and assayed for *Rev-erba* and *Nfil3* expression in intestinal epithelial cells. Consistent with our in vitro findings, the *Stat3^{ΔIEC}* mice showed increased expression of epithelial *Rev-erba* and decreased expression of *Nfil3* as compared with their *Stat3^{f1/f1}* littermates (Fig. 3, G and H). The expression of *Stat3* and the activation of STAT3 in intestinal epithelial cells did not exhibit diurnal rhythms (fig. S10, A and B), indicating that STAT3 does not generate the rhythmicity in *Rev-erba* and *Nfil3* expression. Instead, our findings suggest that diurnal rhythms in NFIL3 expression are generated by the circadian clock through REV-ERB α , whereas the amplitude of these rhythms is fine-tuned by the microbiota through STAT3.

To understand the mechanism by which epithelial NFIL3 regulates fat storage and body composition, we compared the transcriptomes of epithelial cells from *Nfil3^{f1/f1}* and *Nfil3^{ΔIEC}* mice. We performed an RNA sequencing analysis on intestinal epithelial cells at multiple time points across the 24-hour day-night light cycle. We identified 33 transcripts that have differential abundances in *Nfil3^{f1/f1}* and *Nfil3^{ΔIEC}* mice, noting that expression of a number of these genes was diurnally rhythmic in *Nfil3^{f1/f1}* mice (Fig. 4A). Rhythmic expression of the clock genes *Bmal1* (*Arntl*), *Per2*, and *Nr1d1* (*Rev-erba*) was maintained in *Nfil3^{ΔIEC}* mice (Fig. 4A), indicating that the core clock mechanism remains intact. Seventeen of the transcripts encoded proteins that are known to function in lipid uptake and metabolism (Fig. 4A). These included *Cd36*, encoding a transporter that imports dietary fatty acids into cells (23); *Scd1*, encoding a stearoyl-coenzyme A-desaturase 1 (24); *Cyp2e1*, encoding a fatty acid hydroxylase (25); and *Fabp4*, encoding a fatty acid binding protein (26). Deletion of each of these genes protects against HFD-induced obesity and/or insulin resistance (24–27), suggesting that their lowered expression in *Nfil3^{ΔIEC}* mice

could partially account for the metabolic phenotypes of these mice.

We further analyzed *Cd36* and *Scd1* transcripts by quantitative real-time polymerase chain reaction (qRT-PCR), confirming that expression of both genes required epithelial NFIL3 and the microbiota (Fig. 4B). Western blot analysis confirmed that CD36 protein levels were reduced in germ-free and *Nfil3^{ΔIEC}* mice (Fig. 4C). Additionally, expression of *Cd36* and *Scd1* was reduced in *Id2^{gfp/gfp}* and *Stat3^{ΔIEC}* mice (Fig. 4, D and E), consistent with microbiota regulation of *Nfil3* expression through ILC and epithelial STAT3. Thus, the microbiota regulates an NFIL3-dependent lipid metabolic program that is intrinsic to intestinal epithelial cells.

These findings accord with the key functions of intestinal epithelial cells in fatty acid uptake and metabolism. After absorption by enterocytes, fatty acids are processed and packaged into chylomicrons for export into the circulation. These processes show circadian rhythmicity, which results in diurnal variations in circulating lipids (28). Additionally, disruption of rhythms in chylomicron export, as seen in mice lacking nocturnin, is also associated with a lean phenotype (29). Thus, we hypothesized that the metabolic phenotypes of *Nfil3^{ΔIEC}* mice might arise from reduced epithelial cell uptake and processing of dietary lipids with consequent lowered export of lipids to the circulation for storage in adipose tissue.

We tested this idea by visualizing lipid stores in small intestinal tissues from HFD-fed *Nfil3^{ΔIEC}* and *Nfil3^{f1/f1}* mice. Lipids were detected by staining small intestinal sections with Oil Red O, which revealed that the intestinal epithelial cells of *Nfil3^{f1/f1}* mice harbor abundant lipids (Fig. 4F). By contrast, lipids were less abundant in intestinal epithelial cells from *Nfil3^{ΔIEC}* mice (Fig. 4F). *Nfil3^{ΔIEC}* mice also showed reduced Oil Red O staining in subepithelial intestinal tissues, suggesting reduced export of lipids into the lymphatic capillaries that transport packaged lipids to the bloodstream (fig. S11). Consistent with these findings, lipid concentrations were also lower in intestinal epithelial cells (Fig. 4G) but higher in feces (Fig. 4H) from *Nfil3^{ΔIEC}* mice as compared with *Nfil3^{f1/f1}* mice. Thus, epithelial NFIL3 regulates lipid absorption and export in intestinal epithelial cells, potentially explaining why *Nfil3^{ΔIEC}* mice have a limited body-fat gain on a HFD.

Here we have shown that NFIL3 is an essential molecular link among the microbiota, the circadian clock, and host metabolism. Our findings indicate that the microbiota acts through NFIL3 to regulate lipid uptake and storage, thus providing insight into how the intestinal microbiota regulates host metabolism and body composition. Further, we have shown that the ILC3-STAT3 signaling relay forms an essential conduit between the microbiota and the epithelial circadian clock, thus identifying key molecular circuitry through which the microbiota interacts with the clock (fig. S12). These results potentially provide a deeper understanding of why perturbing

microbiota-clock interactions can lead to metabolic disease (4, 5). Our studies could also help to explain why circadian clock disruptions in humans, arising from shift work or international travel, are associated with an increased occurrence of metabolic diseases, including obesity, diabetes, and cardiovascular disease (30, 31). Ultimately, our findings could lead to new strategies for treating metabolic disease by targeting NFIL3, STAT3, the microbiota, or the circadian clock.

REFERENCES AND NOTES

1. M. Ng et al., *Lancet* **384**, 766–781 (2014).
2. F. Bäckhed et al., *Proc. Natl. Acad. Sci. U.S.A.* **101**, 15718–15723 (2004).
3. P. J. Turnbaugh et al., *Nature* **444**, 1027–1031 (2006).
4. C. A. Thaiss et al., *Cell* **159**, 514–529 (2014).
5. V. Leone et al., *Cell Host Microbe* **17**, 681–689 (2015).
6. X. Yu et al., *Science* **342**, 727–730 (2013).
7. X. Yu et al., *eLife* **3**, e04406 (2014).
8. A. Mukherji, A. Kobiita, T. Ye, P. Chambon, *Cell* **153**, 812–827 (2013).
9. S. Mitsui, S. Yamaguchi, T. Matsuo, Y. Ishida, H. Okamura, *Genes Dev.* **15**, 995–1006 (2001).
10. H. Duez et al., *Gastroenterology* **135**, 689–698.e5 (2008).
11. S. Vaishnava et al., *Science* **334**, 255–258 (2011).
12. S. Jung et al., *Immunity* **17**, 211–220 (2002).
13. S. L. Sanos et al., *Nat. Immunol.* **10**, 83–91 (2009).
14. T. Sano et al., *Cell* **163**, 381–393 (2015).
15. G. F. Sonnenberg, L. A. Fouser, D. Artis, *Adv. Immunol.* **107**, 1–29 (2010).
16. M. D. Boos, Y. Yokota, G. Eberl, B. L. Kee, *J. Exp. Med.* **204**, 1119–1130 (2007).
17. A. K. Savage et al., *Immunity* **29**, 391–403 (2008).
18. S. Sawa et al., *Nat. Immunol.* **12**, 320–326 (2011).
19. G. Eberl et al., *Nat. Immunol.* **5**, 64–73 (2004).
20. M. A. Kinnebrew et al., *Immunity* **36**, 276–287 (2012).
21. J. M. Pickard et al., *Nature* **514**, 638–641 (2014).
22. C. A. Lindemans et al., *Nature* **528**, 560–564 (2015).
23. C. T. Coburn et al., *J. Biol. Chem.* **275**, 32523–32529 (2000).
24. P. Cohen et al., *Science* **297**, 240–243 (2002).
25. H. Zong, M. Armoni, C. Harel, E. Karnieli, J. E. Pessin, *Am. J. Physiol. Endocrinol. Metab.* **302**, E532–E539 (2012).
26. G. S. Hotamisligil et al., *Science* **274**, 1377–1379 (1996).
27. L. Cai, Z. Wang, A. Ji, J. M. Meyer, D. R. van der Westhuyzen, *PLOS ONE* **7**, e36785 (2012).
28. X. Pan, M. M. Hussain, *J. Lipid Res.* **50**, 1800–1813 (2009).
29. N. Douris et al., *Curr. Biol.* **21**, 1347–1355 (2011).
30. O. M. Buxton et al., *Sci. Transl. Med.* **4**, 129ra43 (2012).
31. F. A. J. L. Scheer, M. F. Hilton, C. S. Mantzoros, S. A. Shea, *Proc. Natl. Acad. Sci. U.S.A.* **106**, 4453–4458 (2009).

ACKNOWLEDGMENTS

We thank C. L. Behrendt-Boyd, T. Leal, and B. Hassell for assistance with mouse experiments and other members of the Hooper laboratory for discussions and critical reading of the manuscript. This work was supported by NIH grant R01 DK070855 (L.V.H.), a Burroughs Wellcome Foundation Investigators in the Pathogenesis of Infectious Diseases Award (L.V.H.), the Welch Foundation (L.V.H.), and the Howard Hughes Medical Institute (L.V.H.). All data and code to understand and assess the conclusions of this research are available in the main text, supplementary materials, and via the Gene Expression Omnibus repository with accession number GSE1100339.

SUPPLEMENTARY MATERIALS

www.sciencemag.org/content/357/6354/912/suppl/DC1
Materials and Methods
Figs. S1 to S12
Table S1
References (32–37)

28 February 2017; accepted 7 August 2017
10.1126/science.aan0677

The intestinal microbiota regulates body composition through NFIL3 and the circadian clock

Yuhao Wang, Zheng Kuang, Xiaofei Yu, Kelly A. Ruhn, Masato Kubo and Lora V. Hooper

Science **357** (6354), 912-916.
DOI: 10.1126/science.aan0677

Light, fat, and commensals

The gut microbiota facilitates energy harvest from food and transfers it into fat storage. Working in mice, Wang *et al.* found that an epithelial cell circadian transcription factor, NFIL3, is involved in regulating body composition through lipid uptake. Flagellin and lipopolysaccharide produced by certain microbes tuned the amplitude of oscillation of NFIL3 through innate lymphoid cell (ILC3) signaling, STAT3, and the epithelial cell clock. Such interactions may help to explain why circadian clock disruptions in humans, arising from shift work or international travel, frequently track with metabolic diseases, including obesity, diabetes, and cardiovascular disease.

Science, this issue p. 912

ARTICLE TOOLS

<http://science.sciencemag.org/content/357/6354/912>

SUPPLEMENTARY MATERIALS

<http://science.sciencemag.org/content/suppl/2017/08/31/357.6354.912.DC1>
<http://science.sciencemag.org/content/suppl/2017/08/31/357.6354.912.DC2>

RELATED CONTENT

<http://stm.sciencemag.org/content/scitransmed/9/379/eaaf6397.full>
<http://stm.sciencemag.org/content/scitransmed/9/376/eaaf9655.full>
<http://stm.sciencemag.org/content/scitransmed/9/376/eaaf9412.full>
<http://stm.sciencemag.org/content/scitransmed/9/390/eaal4069.full>

REFERENCES

This article cites 37 articles, 13 of which you can access for free
<http://science.sciencemag.org/content/357/6354/912#BIBL>

PERMISSIONS

<http://www.sciencemag.org/help/reprints-and-permissions>

Use of this article is subject to the [Terms of Service](#)